Supporting Information

Optical Conductivity of Two-Dimensional Silicon: Evidence of Dirac Electrodynamics

Carlo Grazianetti[1], Stefania De Rosa[2], Christian Martella[1], Paolo Targa[3], Davide Codegoni[3], Paola Gori[4], Olivia Pulci[5,6], Alessandro Molle[1,*], Stefano Lupi[2,*]

[1]CNR-IMM Unit of Agrate Brianza, via C. Olivetti 2, Agrate Brianza, I-20864, Italy

[2]CNR-IOM Dipartimento di Fisica, Università di Roma La Sapienza, p.le Aldo Moro 2, Roma, I-00185, Italy

[3]STMicroelectronics, via C. Olivetti 2, Agrate Brianza, I-20864, Italy

[4]Dipartimento di Ingegneria, Università Roma Tre, via della Vasca Navale 79, I-00146, Roma, Italy

[5]Dipartimento di Fisica, Università di Roma Tor Vergata, via della Ricerca Scientifica 1, Roma, I-00133, Italy

[6]INFN, Sezione di Roma Tor Vergata, via della Ricerca Scientifica 1, Roma, I-00133, Italy

*Corresponding Authors: Prof. Stefano Lupi (stefano.lupi@roma1.infn.it) and Dr. Alessandro Molle (alessandro.molle@mdm.imm.cnr.it)

1. Samples characterization

The variable thickness (VT) sample was grown by molecular beam epitaxy (MBE) by imposing a slope in the thickness of the silicon nanosheets (SiNSs). *Ex situ* atomic force microscopy (AFM) shows that the minimum and maximum silicon thicknesses along the sample are 1.5 and 7 nm, respectively. **Figure S1** shows the line profile across the edge of the capped SiNSs and bare Al_2O_3(0001) substrate (see inset). By taking into account the 5 nm-thick amorphous Al_2O_3 grown *in situ* by MBE, we get the real thickness of the SiNSs.

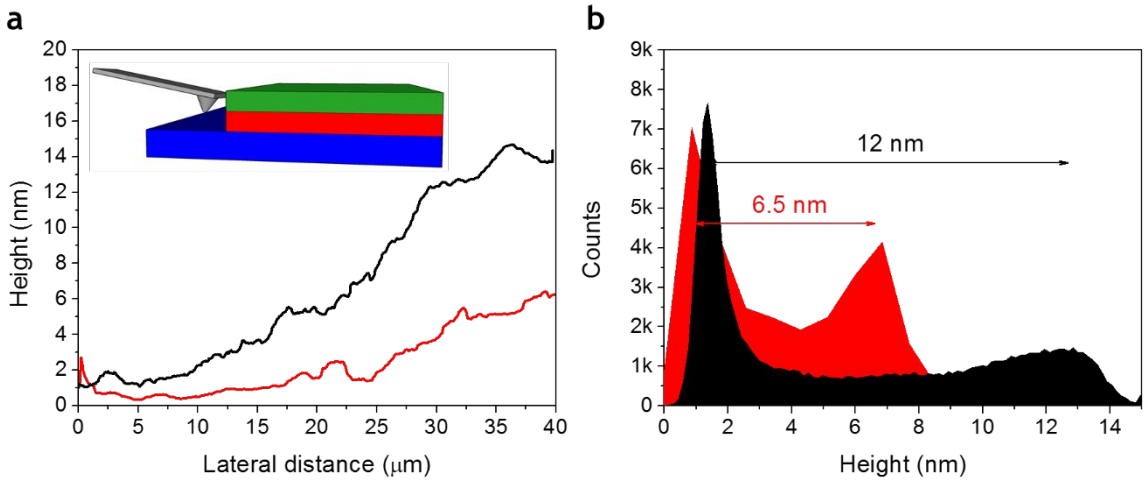

Figure S1. (a) AFM line profiles of the thinnest (red curve) and thickest (black curve) part of the VT sample across the step between the bare substrate and the capped SiNSs. (b) Height counts of the respective curves of (a).

The minimum thickness explored in our survey is 0.5 nm (uniform throughout the sample) SiNS. Such a thickness is beyond the vertical AFM resolution, so the AFM line profile evidences a step of 5 nm that can be fully attributed to the amorphous Al_2O_3 capping layer. **Figure S2** shows the Si 2*p* core level placed at 100.73 eV in agreement with the thinnest part of the VT sample.

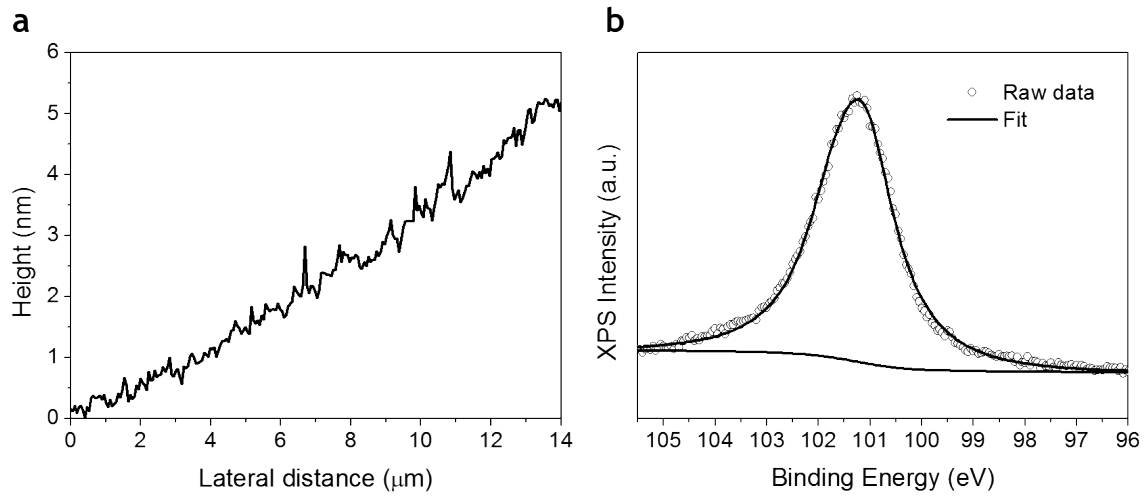

Figure S2. (a) AFM line profile of the CT sample across the step between the bare substrate and the capped SiNS and (b) Si 2*p* core level.

For comparison purpose, a thick (~25 nm) amorphous silicon sample was grown by MBE on Al_2O_3(0001) at room temperature. **Figure S3** shows the AFM profile on the uncapped sample, *i.e.* the total height is the real silicon thickness, and the Si 2*p* core level with binding energy of 98.5 eV.

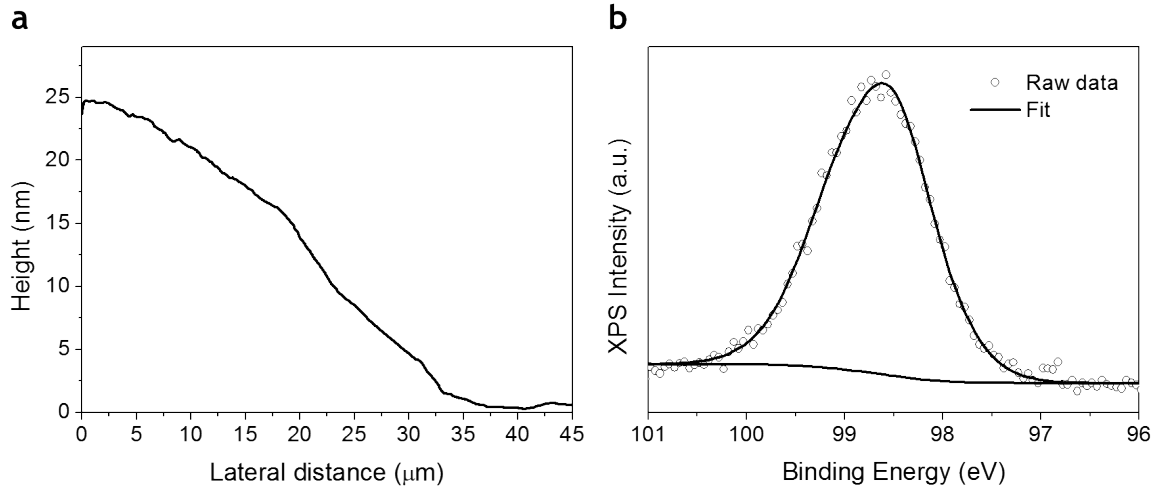

Figure S3. (a) AFM line profile of the reference sample across the step between the bare substrate and the 25 nm-thick silicon film and (b) Si 2*p* core level.

Table S1 reports binding energy (BE) and full width half maximum (FWHM) of Al 2*p* and O 1*s* core levels, before and after silicon deposition in the constant thickness (CT) sample. Although both core levels exhibit a shift to higher BE after silicon deposition, the FWHM is nearly constant thus demonstrating the absence of strong chemical bonds between the SiNSs and the Al_2O_3(0001) substrate.

Core Level	Before silicon		After silicon	
	BE (eV)	**FWHM (eV)**	**BE (eV)**	**FWHM (eV)**
Al 2*p*	74.6	1.33	75.38	1.45
O 1*s*	531.44	1.57	532.02	1.54

Table S1. $Al_2O_3(0001)$ core levels before and after silicon deposition.

2. Energy dispersive x-rays (EDX) maps

Figure S4 reports on the scanning transmission electron microscopy (STEM)-EDX elemental mapping results of the encapsulated SiNSs on $Al_2O_3(0001)$ substrate. The one-element mapping of the chromium, aluminum, silicon, and oxygen (from left to right) along the cross-section cut described in main text as well as the respective line profiles (**Figure 2b** of main text).

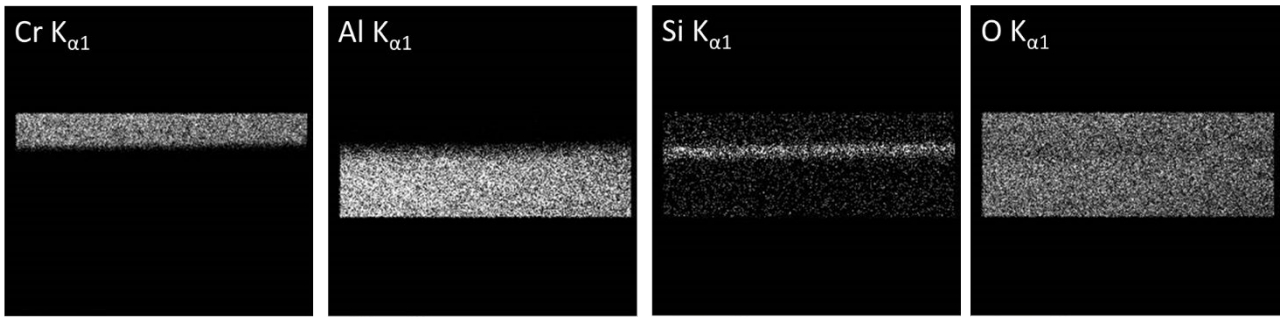

Figure S4. Cross-sectional EDX compositional maps of the chromium, aluminum, silicon, and oxygen, elements of the Cr/a-Al_2O_3/Si/$Al_2O_3(0001)$ stack, respectively.

3. Optical spectroscopy

Kramers-Kronig transformations are typically applied to homogeneous semi-infinite materials. From a single macroscopic transmittance or reflectance spectrum, it is possible to extract any microscopic optical response functions like, for instance, the real and imaginary parts of refraction index, $n(\omega)$ and $k(\omega)$, respectively, the optical conductivity $\sigma(\omega)$, and the dielectric function $\varepsilon(\omega)$. In the present case, the uncertainty on the extracted values depends on the spectral range extension and, as a consequence, of the extrapolation at low and high frequency. For optically stratified systems like thin films on substrate this procedure cannot be utilized. In the past, a fitting procedure has been used in this case in which the optical properties of films are described through the use of a

Drude-Lorentz model of the optical conductivity (refraction index/dielectric function) and the optical properties of the substrate are independently measured and used as input parameters in the fitting procedure. Although this procedure provides good results in many materials,[1] the real and imaginary parts of any microscopic response function are not related, in principle, by a causality relationship and their values may depend on the specific used optical model. Recently, a model independent, Kramers-Kronig constrained fitting procedure has been developed and now routinely used on various 2D and 3D materials.[2] All microscopic optical data in the main text have been obtained by such RefFIT program. Moreover, let us notice that the transmittance of SiNSs and pure Al_2O_3(0001) substrate have been measured in a very broad spectral range (from 0.25 to 4.5 eV). This range not only covers all the relevant expected electronic excitations of SiNSs but also strongly reduces possible spurious extrapolation effects on microscopic quantities. In **Figure S5** comparison between the real and imaginary parts (*n* and *k*) of the refraction index of Al_2O_3(0001) as extracted from RefFIT program and literature data is reported.[3] The very good superposition supports the reliability of this Kramers-Kronig constrained method in the analysis of microscopic optical data of SiNSs from the optical transmittance (see **Figure S6**).

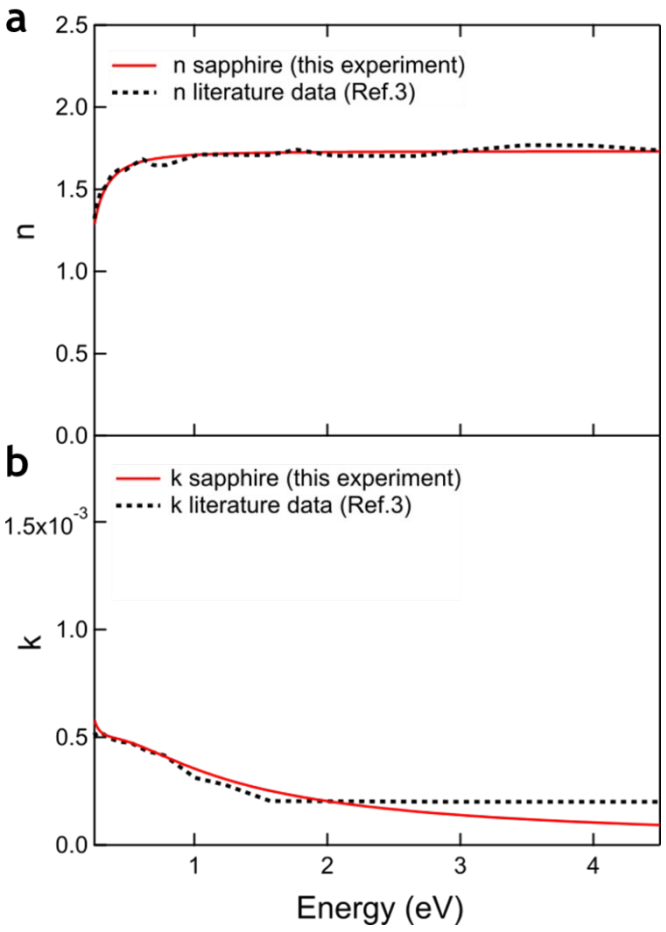

Figure S5. (a) Real part of the refraction index of Al_2O_3(0001) substrate extracted through transmittance data (red curve) compared with reference (black dotted curve) in the measured photon range from 0.25 to 4.5 eV. (b) Imaginary part of the refraction index of Al_2O_3(0001) substrate as for (a).

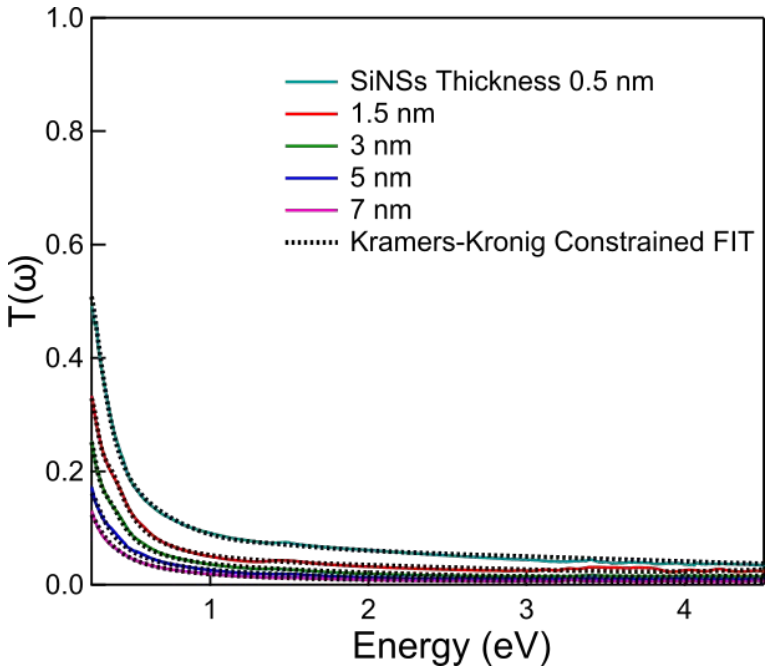

Figure S6. The optical transmittance of SiNSs on Al_2O_3(0001) substrate (solid curves) is shown in the spectral range from 0.25 to 4.5 eV. The Kramers-Kronig constrained fitting obtained through the RefFIT program are indicated by black dashed lines.

4. Density functional theory (DFT) modelling

Structural properties

Two categories of adsorption configurations can be grouped as the result of the geometry optimization: SIS (Strongly-Interacting Silicene) and WIS (Weakly-Interacting Silicene). The most stable configurations belong to the SIS class. The one that has the lowest energy is shown in **Figure S7**.

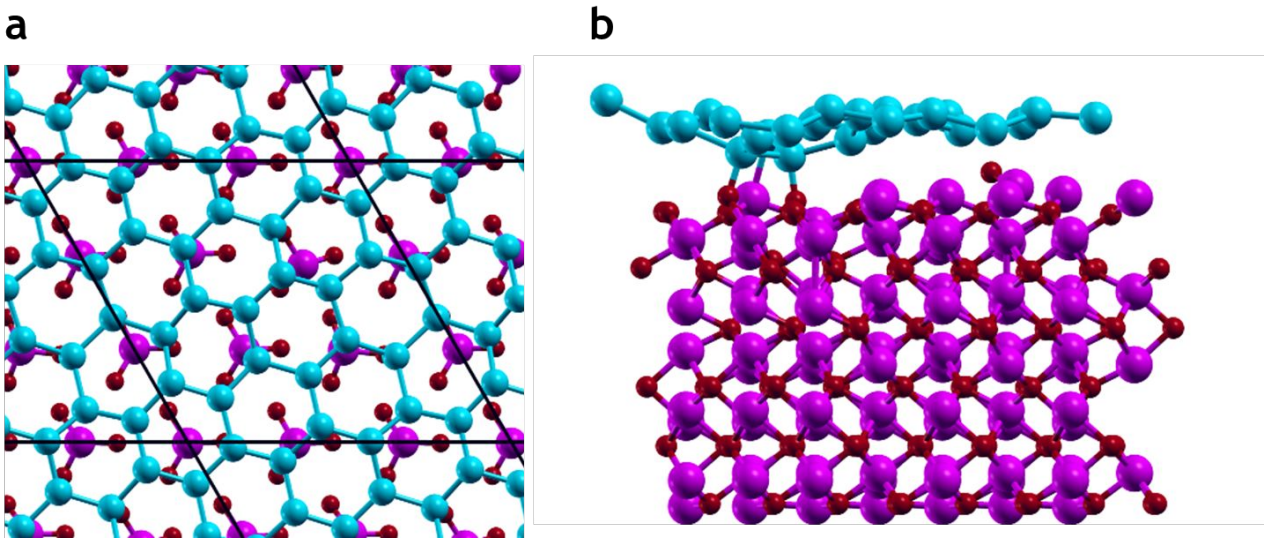

Figure S7. (a) Top view of the most stable SIS configuration (cyan is silicon, magenta is aluminum, and red is oxygen, whereas black lines highlight the surface unit cell; only the upper Al_2O_3(0001) layer is reported for clarity). (b) Side view.

It can be observed that, although the honeycomb appearance of the silicene sheet is preserved, there is a significant interaction with the substrate and silicon atoms show a spread of heights above the substrate (the largest difference in height between the silicon atoms being 2.09 Å, with an average buckling of 0.72 Å). In addition, also the upper layer of the substrate is quite distorted with a few oxygen atoms that tend to bond to silicon atoms. The average distance between the silicon layer and the uppermost Al_2O_3 layer is 2.8 Å. These geometrical distortions have profound effect on the electronic properties of the system, and on its optical response. The Dirac cone disappears, a gap opens, and no infrared (IR) constant behavior of the absorbance survives.

An example of a WIS geometry is reported in **Figure S8**.

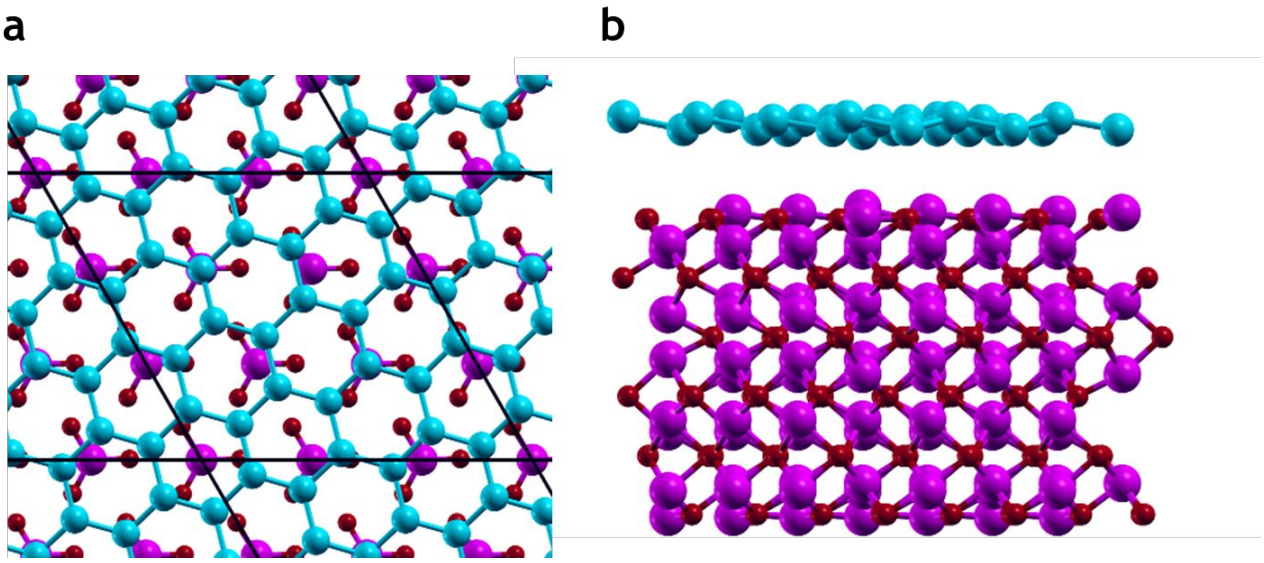

Figure S8. (a) Top view of the most stable WIS configuration (cyan is silicon, magenta is aluminum, and red is oxygen, whereas black lines highlight the surface unit cell; only the upper Al_2O_3(0001) layer is reported for clarity). (b) Side view.

It is clear that in this case the appearance of the silicon layer is much closer to that of freestanding silicene. The largest difference in height of the silicon atoms is 0.63 Å with an average buckling of 0.42 Å (to be compared with the 0.44 Å buckling of the freestanding ideal silicene). The average distance between the silicon layer and the uppermost Al_2O_3 layer is 3.3 Å.

The interaction of the silicene layer with the substrate is weak in the WIS class of geometries. As a consequence, there are several configurations that are essentially degenerate in energy with a negligible dependence on the relative in plane positions of silicene layer and substrate. In all cases, the Dirac cone survives (although a small gap appears) and the constant universal IR behavior of the absorbance is preserved (for energies larger than the gap).

The properties of SIS and WIS structures are summarized in **Table S2**.

Configuration	E_B (eV/Si atom)	E_{gap} (eV)	Bond length *l* (Å)
SIS	0.16	0.39 (indirect K→Γ) 0.44 (direct K)	2.33< *l*<2.53
WIS	0.09	0.05 (direct K)	2.34< *l*<2.37

Table S2. Binding energy (E_B), bandgap (E_{gap}), and bond length *l* for the calculated silicene geometries on $Al_2O_3(0001)$.

Optical properties

Previous calculations[4] on freestanding silicene, performed within the GW approximation and with the inclusion of excitons, have shown a cancellation between the quasiparticle effects and the electron-hole attraction, hence suggesting that DFT gives quite reliable results. The 2D-conducibility (conductance) was calculated starting from the imaginary part of the dielectric function ε_2 of the system. We call ε^{SL} the dielectric function of the superlattice (vacuum plus slab material), and ε^{M} the dielectric function of the sample (our slab). The slab is composed by a substrate [$Al_2O_3(0001)$ in our case] and an overlayer (silicon).

Since bulk $Al_2O_3(0001)$ is transparent in the visible and near UV range, any structure in the imaginary part of the dielectric constant ε^{M} will be essentially due to the silicon overlayer and to the surface of the sapphire.

If $\boldsymbol{l}$ is the slab (sample) thickness, $\boldsymbol{L}$ the supercell (superlattice) thickness, it holds:

$$\boldsymbol{L}\varepsilon^{SL} = \boldsymbol{l}\varepsilon^{M} + (\boldsymbol{L}-\boldsymbol{l})$$

We have direct access to ε^{SL} through the Fermi golden rule calculation of the momentum matrix elements between valence and conduction states of our superlattice.

If we take only the imaginary part of the equation above, we get:

$$\boldsymbol{l}\varepsilon_2^{M} = \boldsymbol{L}\varepsilon_2^{SL}$$

Hence the silicon on sapphire dielectric function (multiplied by the thickness $\boldsymbol{l}$) can be calculated directly from the supercell dielectric function. From that, the real part of the 2D optical conductivity (conductance)

$$\sigma_1(\omega) = \omega\, \boldsymbol{l}\, \varepsilon_2^{M}/4\pi$$

is computed and renormalized to the "quantum conductivity" $\sigma_0 = e^2/4\hbar$.

References

(1) Dressel, M.; Gruner, G. *Electrodynamics of Solids*; Cambridge University Press: Cambridge, 2002.

(2) Kuzmenko, A. B. Kramers–Kronig Constrained Variational Analysis of Optical Spectra. *Rev. Sci.*

Instrum. **2005**, *76* (8), 083108.

(3) Palik, E. D. *Handbook of Optical Constants of Solids*; Academic Press, 1998.

(4) Hogan, C.; Pulci, O.; Gori, P.; Bechstedt, F.; Martin, D. S.; Barritt, E. E.; Curcella, A.; Prevot, G.; Borensztein, Y. Optical Properties of Silicene, Si/Ag(111), and Si/Ag(110). *Phys. Rev. B* **2018**, *97* (19), 195407.